J. Chem. Sci., Vol. 117, No. 5, September 2005, pp. 555–560.

Performance of density functional theory methods to describe intramolecular hydrogen shifts

NELLY GONZÁLEZ-RIVAS and ANDRÉS CEDILLO*

Departamento de Química, UAM-Iztapalapa, San Rafael Atlixco 186, Iztapalapa DF 09340, México
e-mail: cedillo@xanum.uam.mx

Abstract. The performance of three exchange and correlation density functionals, LDA, BLYP and B3LYP, with four basis sets is tested in three intramolecular hydrogen shift reactions. The best reaction and activation energies come from the hybrid functional B3LYP with triple-*z* basis sets, when they are compared with high-level post-Hartree–Fock results from the literature. For a fixed molecular geometry, the electrophilic Fukui function is computed from a finite difference approximation. Fukui function shows a small dependence with both the exchange and correlation functional and the basis set. Evolution of the Fukui function along the reaction path describes important changes in the basic sites of the corresponding molecules. These results are in agreement with the chemical behavior of those species.

Keywords. DFT performance; intramolecular hydrogen shifts; Fukui function.

1. Introduction

Chemical compounds present different types of isomerism. When two isomers differ by the placement of an atom or a functional group and an interconversion equilibrium is established, this process is referred as a tautomeric equilibrium and the isomers are known as tautomers.[1,2] Tautomerism arising from a hydrogen shift occurs frequently in many chemical systems, such as keto-enol and imine-enamine equilibrium, aminoacid zwiterionic forms, metabolic intermediates.[3] In these processes an intramolecular proton transfer occurs, where a hydrogen ion jumps from one atom to another atom of the same molecule. The reactions HAB $\leftrightarrow$ ABH and HABC $\leftrightarrow$ ABCH exemplify the 1,2 and 1,3 hydrogen shifts respectively. The study of tautomerism has been very useful in rationalizing some aspects of the chemical bond, mainly because the proton is able to form a chemical bond with two different atoms of the same molecule and, in most of the cases, the stability of both isomers is different.[4] The stability strongly depends on the environment. For aminoacids, the neutral isomer is more stable than the zwiterion in the gas phase, but in aqueous solution the zwiterion is the stable form. In addition, the molecular structure of zwiterions and peptides depends on the acidity of the solution.

In the literature one can find several theoretical studies of tautomerism.[5–8] These studies confirm the established stability trends and they are mainly interested in the energy of the processes.[5,6] In some cases, the transition state for the gas phase reaction is presented and the relationship with the Hammond Principle is also analyzed.[7] The evolution of molecular properties along the reaction path has also been described for some systems with keto-enol equilibrium.[8]

In a tautomeric process, the proton moves from one atom to another. Note that this hydrogen ion can be identified as a Lewis acid, while the protonation site corresponds to a Lewis basic site. During the transfer process, molecular properties evolve, as a consequence of the breaking and formation of chemical bonds, and the reactivity of the molecule changes. Since the proton usually binds to basic sites, it is very important to locate and characterize this kind of reactive sites, as well as their evolution along the process. Density function theory (DFT) provides reactivity parameters[9] which are useful in the understanding of Lewis acid-base behavior of molecules. For a detailed description of the regions of the molecule, the Fukui function is able to locate Lewis acidic and basic sites.[10]

In the present work we analyze of the performance of DFT methods to describe intramolecular hydrogen shifts. Three small molecules (HCl–O, H_2S=O and H_3C–CH=O) were selected to test the ability of three density functionals, with four basis sets, to describe molecular geometries of both tautomers and the cor-

*For correspondence

Table 1. Reaction and activation energies, in kcal mol^{-1}.

			B1	B2	B3	B4	Ref.
H_2SO	HF	ΔE_r	–32·4	–21·6	–32·8	–24·2	–18·3
		$\Delta E^{\dagger}$	53·8	58·4	48·2	55·5	43·7
	LDA	ΔE_r	–21·7	–14·4	–23·7	–17·9	
		$\Delta E^{\dagger}$	38·2	38·6	32·0	36·2	
	BLYP	ΔE_r	–22·3	–15·5	–24·6	–18·8	
		$\Delta E^{\dagger}$	38·8	40·1	33·1	37·6	
	B3LYP	ΔE_r	–25·3	–17·1	–27·0	–20·6	
		$\Delta E^{\dagger}$	41·9	44·0	36·2	41·4	
HClO	HF	ΔE_r	–68·3	–58·7	–62·9	–62·3	–53·4
		$\Delta E^{\dagger}$	17·2	23·5	16·5	21·3	22·7
	LDA	ΔE_r	–61·8	–48·0	–55·0	–50·8	
		$\Delta E^{\dagger}$	21·1	20·6	15·6	18·6	
	BLYP	ΔE_r	–62·5	–50·5	–56·2	–52·7	
		$\Delta E^{\dagger}$	18·6	18·4	13·7	16·6	
	B3LYP	ΔE_r	–65·2	–52·5	–58·4	–54·7	
		$\Delta E^{\dagger}$	15·9	20·3	14·9	18·3	
CH_3CHO	HF	ΔE_r	17·0	12·0	12·1	11·7	10·4
		$\Delta E^{\dagger}$	90·0	85·9	85·6	85·7	70·2
	LDA	ΔE_r	11·7	6·3	6·1	6·1	
		$\Delta E^{\dagger}$	59·0	55·1	54·5	56·0	
	BLYP	ΔE_r	15·6	9·7	9·6	9·6	
		$\Delta E^{\dagger}$	68·0	64·6	63·6	64·5	
	B3LYP	ΔE_r	15·3	9·6	9·6	9·4	
		$\Delta E^{\dagger}$	72·8	68·8	68·0	68·7	

B1: 6-31g(*d*); B2: 6-311++g(3*df*, 3*pd*); B3: aug-cc-*p*VDZ; B4: aug-cc-*p*VTZ; Ref: see description in text

responding transition state and the reaction and activation energy of these processes. Previous works in the literature show that DFT provides good results for energetics, geometries and vibrational frequencies.[6] In addition, the electrophilic Fukui function, f^-, for tautomers and transition states is also computed and its dependence with the computational method is analyzed, as well as the evolution along the reaction. The results are contrasted with post Hartree–Fock values reported in the literature.

2. Methodology

All the results were calculated with NWChem package.[11] A frequency analysis was applied to optimized and transition state geometries to verify the stability criterion. The selected exchange and correlation functionals for DFT Kohn-Sham calculations were LDA,[12] BLYP[13,14] and B3LYP,[14,15] in order to include functionals without and with gradient corrections and a hybrid one. Four basis sets were used with each functional, two Pople's sets, a small one, 6-31g(*d*) (B1), and a large one, 6-311++g(3*df*, 3*pd*) (B2), and two Dunning's sets, aug-cc-pVDZ (B3) and aug-cc-pVTZ (B4). Hartree–Fock results were also included in the comparison with all the basis sets.

A finite differences approximation is used for the calculation of the electrophilic Fukui functions, $f^-(r) = (\partial r(r)/\partial N)_v^- \approx r_N(r) - r_{N-1}(r)$, where r_N and r_{N-1} are the densities of the neutral molecule and the vertical cation, respectively.

3. Results

For each method, a geometry optimization was performed for the tautomers and a saddle point search was made for the transition state. Reaction and activation energies for the three reactions are reported in table 1. Reported geometries were found in the literature for the same species, a CCSD(T)/6-311++g(3*df*,3*pd*) calculation for the reaction HCl-O ↔ Cl–OH;[16] CASSCF/6-311++g(3*df*, 3*pd*) for H_2S=O ↔ HS–OH;[17] and MP2/6-311+g(*d*, *p*) for the keto-enol tautomerism of acetaldehyde, H_3C–CH=O ↔ H_2C=CH–OH.[18] These geometries are used as refer-

Table 2. Relevant geometrical parameters of the optimized structures, distances in angstroms and angles in degrees.

			B3LYP			BLYP		
		Ref.	B2	B3	B4	B2	B3	B4
HCl–O	r_{ClO}	1·568	1·565	1·630	1·587	1·585	1·649	1·606
	r_{HCl}	1·308	1·320	1·331	1·323	1·345	1·359	1·347
	a_{HClO}	107·6	108·1	106·8	107·6	109·0	108·0	108·6
TS	r_{ClO}	1·764	1·761	1·808	1·776	1·778	1·821	1·791
	r_{HCl}	1·314	1·322	1·330	1·324	1·327	1·335	1·328
	a_{HClO}	62·5	65·3	63·0	62·3	64·7	65·9	64·9
Cl–OH	r_{ClO}	1·699	1·700	1·731	1·708	1·736	1·767	1·744
	r_{HO}	0·964	0·967	0·971	0·967	0·978	0·982	0·978
	a_{ClOH}	102·9	103·6	102·8	103·3	102·5	101·8	102·1
H_2S=O	r_{SO}	1·484	1·485	1·537	1·499	1·504	1·555	1·519
	r_{SH}	1·356	1·382	1·398	1·385	1·401	1·420	1·404
	a_{HSO}	108·9	108·6	107·8	108·3	108·8	108·0	108·4
TS	r_{SO}	1·665	1·657	1·711	1·672	1·684	1·734	1·698
	r_{SH}	1·389	1·403	1·410	1·430	1·413	1·418	1·145
	a_{HSO}	104·9	104·5	103·4	104·14	104·9	104·1	104·5
HS–OH	r_{SO}	1·678	1·674	1·715	1·684	1·705	1·745	1·715
	r_{OH}	0·967	0·964	0·968	0·964	0·975	0·978	0·974
	a_{HSO}	106·4	107·8	106·6	107·5	106·7	105·6	106·4
H_3C–CH=O	r_{CO}	1·200	1·202	1·210	1·204	1·215	1·223	1·216
	r_{CC}	1·490	1·501	1·504	1·500	1·511	1·514	1·511
	r_{CH}	1·090	1·093	1·101	1·093	1·093	1·108	1·100
	a_{HCC}	110·6	111·0	111·0	111·1	111·2	111·2	111·2
TS	r_{CO}	1·280	1·276	1·284	1·277	1·293	1·300	1·294
	r_{CC}	1·400	1·408	1·415	1·408	1·415	1·422	1·414
	r_{CH}	1·480	1·502	1·507	1·501	1·520	1·526	1·520
	a_{HCC}	65·05	66·8	66·9	66·8	67·2	67·3	67·2
H_2C=CH–OH	r_{CO}	1·350	1·375	1·381	1·376	1·360	1·366	1·361
	r_{CC}	1·330	1·338	1·347	1·337	1·327	1·337	1·327
	r_{OH}	0·960	0·974	0·978	0·974	0·964	0·967	0·964
	a_{HOC}	108·1	109·2	109·0	109·2	109·8	109·5	109·8

B2: 6-311++g(3*df*, 3*pd*); B3: aug-cc-*p*VDZ; B4: aug-cc-*p*VTZ; Ref: see description in text

ences. Single point calculations were performed on each species with CCSD(T)/6-311++g(3*df*, 3*pd*) method on the reference geometry, in order to have reference energies at the same level of theory. These results are also included in table 1. A comparison of the values from table 1 shows that the small basis set (B1), 6-31*g*(*d*), has the largest deviations from the reference values, while the triple-*z* basis sets, 6-311++g(3*df*, 3*pd*) (B2) and aug-cc-pvtz (B4), provide the best results in the set. On the other hand, BLYP and B3LYP results are closer to the reference values than HF and LDA ones. On the average, B3LYP/6-311++g (3*df*, 3*pd*) method provides the better relative energy values. Table 2 presents relevant geometric parameters from the optimized molecules together with reference values. This table only includes results from BLYP and B3LYP methods, as these methods produce better relative energies. Again, one can note that triple-*z* basis sets, (B2) and (B4), provide better results. In contrast with Durant,[6a] we found that the BLYP functional is able to locate all the transition state structures with all the basis sets and the use of larger basis sets leads to better energy barriers, specifically, for the B3LYP/6-311++g(3*df*, 3*pd*) method the maximum difference with respect to the reference value is –2·4 kcal mol^{-1}. Our results coincide with previous studies on the same molecules where it is shown that DFT geometries are in good agreement with high-level *ab initio* calculations[6] and DFT methods usually underestimate barrier heights.[6,19] However, the hybrid functional results are closer to the reference values.[6]

Table 3. Fukui function M_{ijk} integrals of the transition state of the reaction $H_2S{=}O \leftrightarrow HS{-}OH$, in atomic units.

	B3LYP/B1	B3LYP/B2	B3LYP/B3	B3LYP/B4	HF/B2	LDA/B2	BLYP/B2
M_{100}	0·13	0·10	0·10	0·10	0·09	0·10	0·10
M_{010}	0·05	–0·02	–0·02	–0·02	0·05	–0·04	–0·03
M_{001}	0·08	0·14	0·15	0·14	0·26	0·07	0·09
M_{200}	2·32	2·59	2·60	2·62	2·42	2·65	2·67
M_{110}	–0·07	–0·07	–0·08	–0·07	–0·04	–0·11	–0·09
M_{101}	–0·43	–0·41	–0·42	–0·42	–0·36	–0·42	–0·42
M_{020}	2·95	3·36	3·39	3·39	3·10	3·47	3·48
M_{011}	–0·10	0·05	0·02	0·04	0·34	–0·06	–0·04
M_{002}	5·28	5·95	6·02	5·98	6·05	5·88	5·94

B1: 6-31g(*d*); B2: 6-311++g(3*df*, 3*pd*); B3: aug-cc-*p*VDZ; B4: aug-cc-*p*VTZ

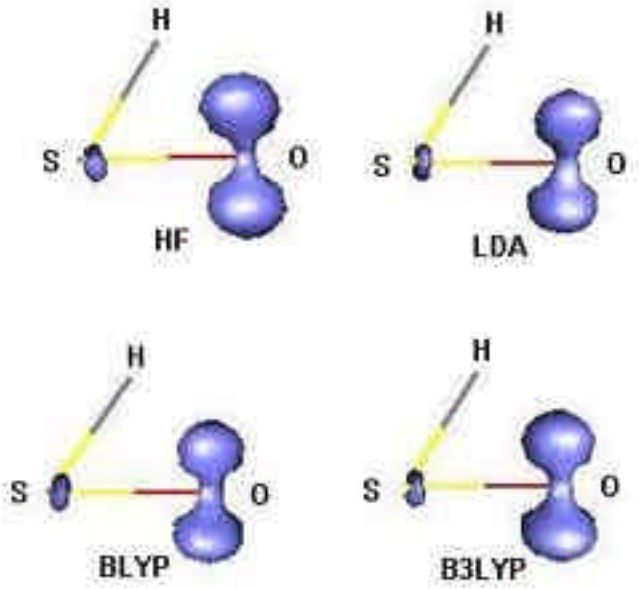

Figure 1. Fukui function f^- isosurfaces (isosurface value: 0·03) of the transition state of the reaction $H_2S = O \leftrightarrow HS{-}OH$, calculated with different methods and the same basis set, 6-311++g(3*df*, 3*pd*).

In order to analyze the dependence of the Fukui function on the computational method, for every method, the Fukui function is calculated for the reference geometries. A quantitative comparison can be made using the moments of the involved densities,

$$M_{ijk} \equiv \int x^i y^j z^k f^-(r)\mathrm{d}r$$

$$= \int x^i y^j z^k \rho_N(r)\mathrm{d}r - \int x^i y^j z^k \rho_{N-1}(r)\mathrm{d}r.$$

Values of the M_{ijk} integrals show a higher dependence on the method, while, for a given method, the basis set has smaller effects. We found that larger variations in M_{ijk} integrals occur in transition states. As a representative case, table 3 presents the values of the M_{ijk} integrals for the transition state of the reaction $H_2S{=}O \leftrightarrow HS{-}OH$. One can note that large basis sets give similar results, on the other hand, DFT methods produce closer values, while HF results are a little farther. The same analysis was made in the moments of the densities, since variations are smaller, they are not tabulated. A graphical comparison of the same cases can be found in figures 1 and 2, where isosurfaces of the Fukui function are represented. The Fukui function is evaluated in a three-dimensional grid, from density grids of the neutral and positive ion. All the isosurfaces are computed at the same positive value. Figure 1 represents the effect of the method on the Fukui function, while in figure 2 the basis set is changed. All the isosurfaces look alike, except for the HF isosurface, which seems to be a little larger. The difference between HF and DFT results is in agreement with the analysis of the values from table 3. This behavior is found to be in agreement with a previous study, [20] where the effect of correlation in the Fukui function is analyzed.

The evolution of the Fukui function for the three reactions is shown in figures 3–5. In figure 3 one can see that, for the reaction $HCl{-}O \leftrightarrow Cl{-}OH$, the reactant's basicity is mainly located at the oxygen atom, but, after the hydrogen shifts from chlorine to oxygen, basicity appears on the chlorine atom and decreases at the oxygen. One can note that oxygen's donating capacity is still larger than chlorine's in the product. In addition, the transition state basicity is mainly located at the oxygen atoms. Figure 4 show a similar behavior for the reaction $H_2S{=}O \leftrightarrow HS{-}OH$, except for the basicity of the product. In HS-OH

molecule, both oxygen and sulfur are singly protonated, but the Fukui function is larger on the sulfur atom, in agreement with the fact that sulfur is more basic than oxygen. For the reaction $H_3C–CH=O \leftrightarrow H_2C=CH–OH$, one can see that, in the reactant, the basic character is manly located at the oxygen of the carbonyl group. At the transition state, the *a*-carbon atom enhances its basicity, while the oxygen basicity decreases. The product shows similar donating capacities on oxygen and *a*-carbon atoms and the orientation of the Fukui function isosurface is normal to the molecular plane, a consequence of the conjugation on the enol.

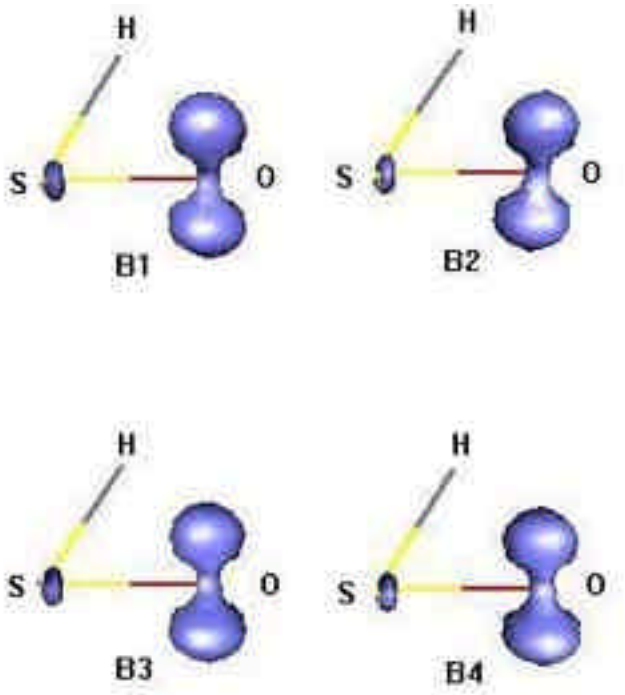

Figure 2. Fukui function f^- isosurfaces (isosurface value: 0·03) of the transition state of the reaction $H_2S= O \leftrightarrow HS–OH$, calculated with different basis sets and the B3LYP method.

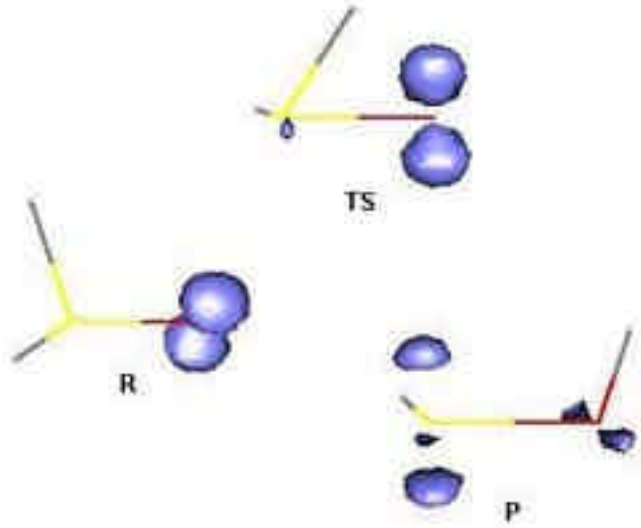

Figure 4. Fukui function f^- isosurfaces (isosurface value: 0·03) of the tautomers and transition state of the reaction $H_2S=O \leftrightarrow HS–OH$, calculated at the B3LYP/6-311++g(3*df*, 3*pd*) level.

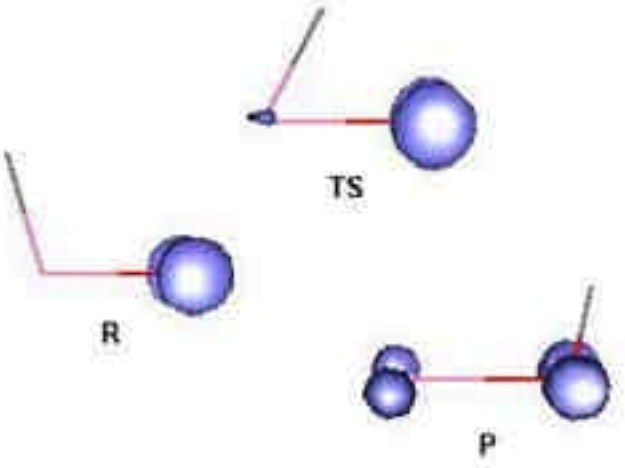

Figure 3. Fukui function f^- isosurfaces (isosurface value: 0·03) of the tautomers and transition state of the reaction $HCl–O \leftrightarrow Cl–OH$, calculated at the B3LYP/6-311++g(3*df*, 3*pd*) level.

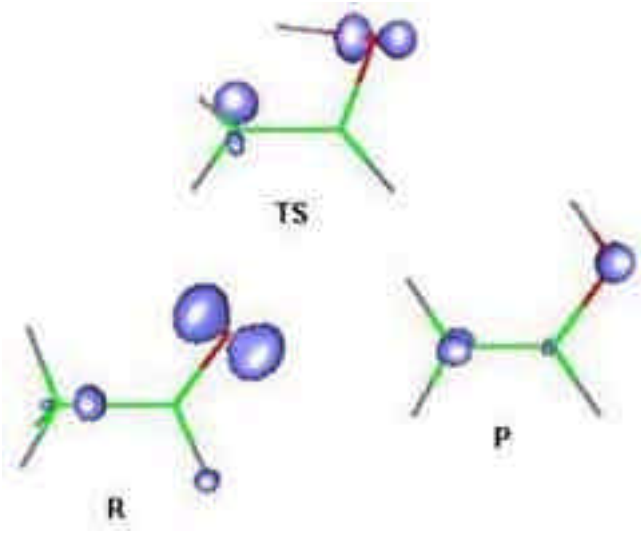

Figure 5. Fukui function f^- isosurfaces (isosurface value: 0·03) of the tautomers and transition state of the reaction $H_3C–CH=O \leftrightarrow H_2C=CH–OH$, calculated at the B3LYP/6-311++g(3*df*, 3*pd*) level.

Comparison of the Fukui function isosurfaces for each reaction shows that the transition state has a closer resemblance to the reactant in figures 3 and 4. With his criterion, both reactions correspond to the Hammond type, in agreement with relative displacement of the proton with respect to both basic sites in the transition state. These results are also in accordance with the Brönsted criterion used earlier.[7] In contrast, the transition state of figure 5 shows no resemblance to any tautomer. Then, for this reaction, the Fukui function isosurface shape does not distinguish between Hammond and anti-Hammond types.

4. Conclusions

In general, DFT Kohn-Sham calculations provide good qualitative descriptions of intramolecular hydrogen shifts when large basis sets are used. Reaction and activation energies calculated with exchange and correlation hybrid functional B3LYP and triple-*z* basis sets are in very good agreement with CCSD(T) energies with the same basis sets. The Fukui function shows a small dependence on the basis set and the exchange and correlation functional. This analysis was made on the value of some integrals (moments) of the Fukui function and graphically, by comparing isosurfaces of the same property.

The evolution of the Fukui function describes the changes of the basic sites of the molecule along the reaction. These changes reflect the chemical nature of the involved species. A visual comparison of the transition state isosurfaces with those from the tautomers allowed us to make a Hammond-like identification in two of the three reactions.

Acknowledgments

Support from CONACYT (México) through a scholarship to NG-R and project funds is gratefully acknowledged. We also thank the Laboratorio de Supercomputo y Visualización en Paralelo (LSVP) at UAM-I for the access to its computer facilities.

References

1. March J 1992 *Advanced organic chemistry: Reactions mechanisms and structure* 4th edn (New York: Wiley)
2. Morrison R T and Boyd R N 1987 *Organic chemistry* 5th edn (Boston: Allyn and Bacon)
3. Cisneros G A, Liu H, Zhang Y and Yang W 2003 *J. Am. Chem. Soc*. **125** 498
4. Beak P 1977 *Acc. Chem. Res*. **10** 186
5. Rak J, Skurski, Simons J and Gutowski M 2001 *J. Am. Chem. Soc*. **123** 11695; Rodriquez C, Cunje A, Shoeib T, Chu I K, Hopkinson A C and Siu K W M 2000 *J. Phys. Chem.* **A104** 5023; Cardenas-Jirón G I and Toro-Labbe A 1997 *J. Mol. Struct.* (*Theochem*) **390** 79; Cardenas-Jirón G I, Lahsen J and Toro-Labbe A 1995 *J. Phys. Chem.* **99** 5325; Cioslowski J 1991 *J. Am. Chem. Soc.* **113** 6756; Wong M W, Wiberg K B and Frisch M J 1992 *J. Am. Chem. Soc.* **114** 1645; Tsuchiya Y, Tamura T, Fuji M and Ito M 1998 *J. Phys. Chem.* **92** 1760; Beak P, Covington J B, Smith S G, White J M and Zeigler J M 1980 *J. Org. Chem.* **45** 1354; Heinrich N, Koch W, Frenking G and Schwarz H 1986 *J. Am. Chem. Soc*. **108** 593
6. (a) Durant J L 1996 *Chem. Phys. Lett.* **256** 595; (b) Torrent M, Duran M and Sola M 1996 *J. Mol. Struct.* (*Theochem*) **362** 163; (c) Poater M, Sola M, Duran M and Robles J 2002 *Phys. Chem. Chem. Phys.* **4** 722; (d) Baker M, Muir M and Andzelm J 1995 *J. Chem. Phys.* **102** 2063
7. Sola M and Toro-Labbe A 1999 *J. Phys. Chem.* **A103** 8847; Bulat F and Toro-Labbe A 2003 *J. Chem. Phys*. **107** 3987
8. Pérez P and Toro-Labbe A 2000 *J. Phys. Chem.* **A104** 1557
9. Parr R G and Yang W 1989 *Density functional theory of atoms and molecules* (New York: Oxford University Press)
10. Parr R G and Yang W 1984 *J. Am. Chem. Soc*. **106** 4049
11. Bernholdt D E *et al* 1995 *Int. J. Quantum Chem. Symp.* **29** 475
12. Vosko S H, Wilk L and Nusair M 1980 *Can. J. Phys.* **58** 1200
13. Becke A D 1988 *Phys. Rev.* **A88** 3098
14. Lee C, Yang W and Par R G 1988 *Phys. Rev*. **B37** 785
15. Becke A D 1993 *J. Chem. Phys.* **98** 5648
16. Jalbout A F 2002 *Mol. Phys*. **24** 3785
17. Cubbage J W and Jenks W S 2001 *J. Phys. Chem.* **A105** 10588
18. Alkorta I and Elguero J 2004 *Tetrahedron Lett.* **45** 4127
19. Barone V and Adamo C 1996 *J. Chem. Phys.* **105** 11007; Zhang Q, Bell R and Truong T N 1995 *J. Chem. Phys.* **99** 592; Jursic B S 1997 *J. Mol. Struct.* (*Theochem*) **417** 89; Thummel H T and Bauschlicher C W 1997 *J. Chem. Phys.* **101** 1188; Bach R D, Glukhovtsev M N and Gonzalez C 1998 *J. Am. Chem. Soc.* **120** 9902; Rice B M, Pai S V and Chabalowski C F 1998 *J. Phys. Chem.* **A102** 6950; Tucker J M and Standard M 1998 *J. Mol. Struct.* (*Theochem*) **431** 193; Jursic B S 1998 *J. Mol. Struct.* (*Theochem*) **430** 17; Yoshizawa K, Shiota Y, Kang S and Yamabe T 1997 *Organometallics* **16** 5058
20. Langenaeker W, De Proft F and Geerlings P 1996 *J. Mol. Struct.* (*Theochem*) **362** 175